[CANCER RESEARCH 63, 4552–4560, August 1, 2003]

Interrogating Androgen Receptor Function in Recurrent Prostate Cancer[1,2]

Liqun Zhang, Mai Johnson, Kim H. Le, Makoto Sato, Romyla Ilagan, Meera Iyer, Sanjiv S. Gambhir, Lily Wu, and Michael Carey[3]

Departments of Biological Chemistry [L. Z., K. H. L., R. I., M. C.] and Urology [M. J., M. S., L. W.], Crump Institute of Molecular Imaging [S. S. G., L. W., M. C.], and Department of Molecular and Medical Pharmacology [M. I., S. S. G.], University of California, Los Angeles, School of Medicine, Los Angeles, California 90095

ABSTRACT

The early androgen-dependent (AD) phase of prostate cancer is dependent on the androgen receptor (AR). However, it is unclear whether AR is fully functional in recurrent prostate cancer after androgen withdrawal. To address this issue we interrogated AR signaling in AD and recurrent prostate cancer xenografts using molecular imaging, chromatin immunoprecipitation, and immunohistochemistry. In the imaging experiments, an adenovirus bearing a two-step transcriptional activation cassette, which amplifies AR-dependent firefly luciferase reporter gene activity, was injected into tumors implanted into severe combined immunodeficiency mice. A charge-coupled device optical imaging system detected the initial loss and then resumption of AR transcriptional activity in D-luciferin-injected mice as tumors transitioned from AD to recurrent growth. The results of chromatin immunoprecipitation and immunohistochemical localization experiments correlated with the Ad two-step transcriptional activation imaging signal. AR localized to the nucleus and bound to the endogenous prostate-specific antigen enhancer in AD tumors but exited the nucleus and dissociated from the enhancer upon castration. However, AR reentered the nucleus and rebound the prostate-specific antigen enhancer as the cancer transitioned into the recurrent phase. Surprisingly, RNA polymerase II and the general factor TFIIB remained bound to the gene throughout the transition. Our data support the concept that AR is fully functional in recurrent cancer and suggest a model by which a poised but largely inactive transcription complex facilitates reactivation by AR at castrate levels of ligand.

INTRODUCTION

Prostate cancer growth is controlled by AR[4] (1), a member of the steroid receptor subfamily of nuclear receptors (2). In the presence of its ligand DHT the bulk of AR moves from the cytoplasm to the nucleus (3, 4), binds to 15-bp DNA elements (AREs) in enhancers and promoters, and activates expression of genes involved in prostate metabolism including PSA.

PSA is a secreted kallikrein protease widely used for evaluating treatment and progression of cancer, although it has some drawbacks in prognostic utility (5). The PSA promoter and enhancer have been delineated and contain AREs necessary for transcriptional activity in AD cancer cell lines such as LNCaP (6–12). A 440-bp core segment of the enhancer plays the major role in androgen responsiveness (10). Multiple dimers of AR bind cooperatively to a cluster of AREs in the core enhancer, and synergistically activate transcription (13, 14) via interaction with coactivators that recruit pol II and its associated factors (1). DHT-dependent binding of AR to the PSA enhancer has been studied extensively in AD LNCaP cells using ChIP but has not yet been evaluated in AD or recurrent tumors (15–17).

A central role for AR in AD prostate cancer has been inferred from the observation that tumor growth initially ceases with treatments that lower the concentration or effectiveness of DHT. Although secreted PSA levels decrease as AR activity is diminished (18), the cancer eventually transitions from the AD state to a recurrent or AI state upon failure of androgen withdrawal therapies (19–21). As the cancer transitions, the levels of secreted PSA rise again, implying that AR is functional.

In many recurrent cancers the AR gene is amplified and/or AR is overexpressed (22, 23). The relevance of AR overexpression in cancer is supported by transgenic animal studies, where forced overexpression of murine AR from the probasin promoter leads to development of high-grade prostatic intraepithelial neoplasia, a precursor to prostate cancer (24). It has been hypothesized that in recurrent cancer, overexpressed AR can function by using castrate levels of DHT or adrenal androgens (22, 25).

Mutations in AR are occasionally associated with recurrent cancer. Certain mutations in the ligand-binding domain of AR permit it to function with alternative ligands in cell culture and *in vivo* (21). Additionally, somatic mutations identified in the transgenic adenocarcinoma of mouse prostate model revealed a correlation between reduced androgen dependence and the presence of mutations in AR functional domains known to interact with coactivators (26). In summary, it is plausible that mutation of AR facilitates interactions with coactivators in the absence of ligand or the presence of alternative ligands.

MAPK has also been postulated to augment AR activity in the absence of ligand (19–21, 27–29). Elevated MAPK levels have been observed in advanced prostate cancer specimens from patients and in recurrent xenograft models (30, 31). Several receptor tyrosine kinases or growth factors that signal through MAPKs activate AR-responsive reporter genes in an AI manner when overexpressed in cell culture (19–21, 27–29). A receptor tyrosine kinase inhibitor that targets the epidermal growth factor receptor pathway inhibits AR activity and tumor growth in animal models (31).

Additional support for a direct role of AR in recurrent cancer growth comes from cell culture studies. Lowering AR levels in an AI LNCaP cell line by injection of an AR-targeted hammerhead ribozyme or AR antibodies reduces cell proliferation (32). It has been suggested that AR may function not by binding DNA but through cytoplasmic interaction with signaling molecules that activate the MAPK pathway (33, 34). However, the effect of AR on PSA gene transcription in at least one AI cell line probably involves DNA

Received 3/13/03; accepted 5/27/03.

The costs of publication of this article were defrayed in part by the payment of page charges. This article must therefore be hereby marked *advertisement* in accordance with 18 U.S.C. Section 1734 solely to indicate this fact.

[1] Supported by Department of Defense Grant PC020177 (to M. C.), CaPCURE Grant (to M. C. and S. S. G.), Department of Defense CDMRP PC000046 (to L. W.), Department of Defense PC991019 (to Charles Sawyers, UCLA School of Medicine, and M. C.), an interdisciplinary seed grant from the Jonsson Comprehensive Cancer Center (to M. C., L. W., and S. S. G.), R01 CA82214 (to S. S. G.), SAIRP R24 CA92865 (to S. S. G.), and Department of Energy Contract DE-FC03-87ER60615 (to S. S. G.). L. Z. is supported by United States Department of Health and Human Services Institutional National Research Service Award #T32CA09056. R. I. is supported by a Research Training in Pharmacological Sciences Award #T32JM08652.

[2] Supplementary data for this article are available at *Cancer Research Online* (http://cancerres.aacrjournals.org).

[3] To whom requests for reprints should be addressed, at Department of Biological Chemistry, University of California Los Angeles School of Medicine, Los Angeles, CA 90095-1737. Phone: (310) 206-7859; Fax: (310) 206-9598; E-mail: mcarey@mednet.ucla.edu.

[4] The abbreviations used are: AR, androgen receptor; ARE, androgen response element; AD, androgen-dependent; ADc, androgen-dependent castrated; AI, androgen-independent; CCD, charge coupled device; CHIP, chromatin immunoprecipitation; DHT, dihydroxytestosterone; LAPC, Los Angeles prostate cancer; MAPK, mitogen-activated protein kinase; pol II, RNA polymerase II; PSA, prostate-specific antigen; SCID, severe combined immunodeficiency; TSTA, two-step transcriptional activation; pfu, plaque-forming unit(s); CMV, cytomegalovirus; Ad, adenovirus; MOI, multiplicity of infection.

binding, because the PSA enhancer requires some of its natural AREs for activity, although other transcription factors also contribute (35).

Despite these intriguing cell culture studies, direct measures of AR activity and binding of AR to responsive genes have not been demonstrated in recurrent tumors. This is an important issue for developing pharmaceuticals targeted to recurrent cancer, the most deadly form of the disease in men. The goal of our study was to confirm AR function in the context of human xenograft tumors implanted into SCID mice. We used the LAPC9 model, a human prostate cancer derived from a bone metastasis (36). LAPC9 tumors express PSA and wild-type AR, and on castration of the SCID mice, the tumor transiently halts growth and gradually transitions into the recurrent state. Continued passage of the tumor in castrated mice generates a stable AI model, which expresses AR and PSA.

We used four tools to study AR function in the LAPC9 tumors: secreted PSA levels, immunohistochemistry, ChIP, and molecular imaging. The PSA levels permitted us to confirm that the tumor responded to androgen deprivation in castrated animals and rose during transition to recurrent cancer. Immunohistochemistry allowed us to monitor nuclear localization, an important parameter of AR function. ChIP enabled us to directly monitor specific AR binding to the endogenous PSA gene within tumors. Gene expression-based molecular imaging is a new technology that permitted us to noninvasively visualize transcriptional activity during cancer progression (37–40).

The molecular imaging technology uses a cooled CCD camera, which detects light emitted from living animals when a firefly luciferase reporter gene is expressed in the presence of its substrate D-luciferin (41). The short half-life of luciferase in combination with highly active reporter genes facilitates dynamic measurements of expression occurring over weeks within tumors implanted into an animal (42). Our imaging system is based on the PSA regulatory region because of its AR responsiveness and prostate specificity (9).

In a previous study, we duplicated the core PSA enhancer and significantly augmented AR-responsive firefly luciferase activity in cell culture (43). An adenovector bearing this imaging cassette, AdPBC, detected distal metastatic lesions in xenograft models using the CCD optical imaging system (44). The overall activity of the AdPBC reporter cassette was only 5% that of AdCMV-luciferase, the benchmark for CCD imaging studies, making it difficult to dynamically monitor the androgen response. To additionally improve the signal we used the TSTA strategy. The duplicated PSA regulatory region was linked to the gene for the potent transcription activator GAL4-VP16. When GAL4-VP16 is synthesized it acts on a GAL4-responsive firefly luciferase reporter gene resulting in amplified levels of expression (45). We previously optimized the system by varying the numbers of GAL4 sites and VP16 activation domains (46).

In this paper we incorporated the optimal TSTA system into a replication-deficient adenovirus (47) to create AdTSTA. Adenovirus exhibits a high infection efficiency and is widely used in gene transfer studies in animals and humans (48). We injected AdTSTA into LAPC9 AD and recurrent tumors implanted into the flanks of SCID mice, and imaged the activation, inactivation, and reactivation of AR activity during cancer progression. Immunohistochemical staining and ChIP of AR on the PSA regulatory region in the various stages of cancer growth supported the concept that AR is fully active in recurrent cancer. ChIP data also suggested a model whereby the RNA pol II transcription complexes on AR-responsive genes do not disappear in the absence of androgen but remain poised to resume activity.

MATERIALS AND METHODS

Adenovirus Constructs. AdTSTA was generated from the optimal TSTA plasmid (46). A second *Not*I site 5′ from the PBC enhancer was removed to create unique *Not*I site in the vector. A *Sal*I-*Not*I fragment containing the core BCVP2G5-Luc fragment was excised by *Not*I and partial *Sal*I digestion, and inserted into the *Sal*I-*Not*I site of pShuttle (Q-Biogene, Carlsbad, CA), which was then incorporated into the adenovirus vector AdEasy through homologous recombination. AdCMV was generated as described previously (44). The viruses were packaged and propagated in 293A cells. The virus was scaled up, purified via a CsCl gradient, and titered by plaque assays on 293 monolayers (infectious units = plaque-forming units). Virus was stored at $\sim 10^{11}$pfu/ml in 10 mM Tris-HCl, 1 mM $MgCl_2$, and 10% glycerol. TSTA plasmid vectors that contain convenient restriction sites for removing PBC and replacing it with any promoter have been constructed and will be provided on request.

Cell Culture and Xenografts. The human prostate cancer cell line LNCaP was grown in RPMI 1640 supplemented with 10% fetal bovine serum and 1% penicillin/streptomycin solution. HeLa, MCF-7, and HepG cells were cultured in DMEM with 10% fetal bovine serum and 1% penicillin/streptomycin. Before transfection, cells were transferred for 24 h into medium containing 5% charcoal-stripped serum (Omega Sci., Tarzana, CA). The synthetic androgen methylenetrienolone (R1881; NEN Life Science Products, Boston, MA) was added to "ligand-positive" samples where indicated.

Human prostate tumor xenografts were generated on SCID mice as described previously (36). Briefly, $\sim 1 \times 10^6$ LAPC-9 tumor cells generously provided by Dr. Charles Sawyers (UCLA School of Medicine, Los Angeles, CA) were mixed 1:1 with Matrigel (BD Scientific) and implanted s.c. on the left flank of male SCID (C.B. −17 *Scid*/*Scid*) mice. The AI sublines were passaged several rounds in castrated male mice. Single-cell suspension cultures were maintained on Pre-BM/GM medium (Clonetics, Walkersville, MD). Alternatively, tumors were extracted from founder mice, minced into ~0.2-mm cubes, bathed in Matrigel, and implanted s.c. onto the left flanks of SCID mice.

Virus Activity Assays. For firefly luciferase assays, the cultured cells were infected with AdTSTA or AdCMV at a MOI of 0.1. After 48 h, the cells were harvested and lysed using the passive lysis buffer provided in the firefly luciferase assay kit (Dual-Reporter Luciferase Assay System; Promega, Madison, WI). Firefly luciferase activities of 5% of the cell lysates supplemented with 100 μl of D-luciferin were measured using a luminometer (Lumat 9507; (Berthold Technologies, Oak Ridge, TN) with an integration time of 10 s.

Immunoblot Analysis of GAL4-VP16 Expression. LNCaP cells were grown in 10-cm dishes and infected with AdTSTA at MOI 10. Forty-eight h later the cells were harvested and lysed with radioimmunoprecipitation assay buffer (10 mM Tris-HCl, 150 mM NaCl, 0.1% SDS, 1% DOC, 1 mM EDTA, and 1% NP40). Protein concentrations of the extracts were normalized (Bio-Rad Dc protein assay kit), and the samples were fractionated on 4–15% gradient acrylamide gels (Bio-Rad, Hercules, CA) and subjected to immunoblot analysis with rabbit polyclonal antibodies generated against intact GAL4-VP16 or loading control proteins.

CCD Imaging of Firefly Luciferase Expression. For the naïve mice, 10^7 pfu of AdTSTA or AdCMV suspended in 100 μl PBS was injected via the tail vein. For the LAPC9 xenografts, a total of 10^7 pfu of AdTSTA or AdCMV in 40 μl PBS was injected directly into the 0.5-cm diameter tumor xenografts at multiple locations. To ensure adequate distribution throughout the tumor, the injection was carried out twice on 2 sequential days. The virus was allowed to express the encoded genes and distribute throughout the tissue for 3–4 days before imaging. At the days specified in the figures, the mice were anesthetized and injected with ~150 mg/kg D-luciferin (~3 mg/mouse). Light signals (CCD images) were obtained using a cooled IVIS CCD camera (Xenogen, Alameda, CA), and images were analyzed with IGOR-PRO Living Image Software, which generates a pseudoimage with an adjustable color scale. We determined the maximum photons/second of acquisition/cm^2 pixel/steridian within a region of interest to be the most consistent measure for comparative analysis. The imaging results correlated closely with luminometry of tissue extracts. Typically our acquisition times ranged from 1 to 10 s.

Tumor Immunohistochemical Analysis. Immunohistochemistry was performed on paraffin-embedded tumor sections with antigen retrieval. Tissue sections were incubated at 4°C overnight with anti-AR 5 μg/ml (UpState, Charlottesville, VA). After stringent blocking, washing, and incubation with

multilink (BioGenex, San Ramon, CA), and alkaline phosphatase label for 20 min at room temperature, sections were washed and developed according to the manufacturer's instructions (BioGenex).

Secreted PSA and Serum DHT Measurements. Blood was withdrawn from the mice by retro-orbital bleeding, and plasma was collected. PSA levels were measured using a PSA ELISA kit (American Qualex, San Clemente, CA), whereas the DHT levels were measured using a DHT ELISA kit (Alpha Diagnostic International, San Antonio, TX). All of the measurements were performed in triplicate.

Tumor Chromatin Immunoprecipitation. Tumors were extracted from the mice and washed with ice-cold PBS. The tumors were quickly minced and immersed in 1% formaldehyde solution, where they were additionally minced and homogenized using a glass dounce. The total incubation in formaldehyde solution was for 30 min. Before sonication, the cell suspensions were washed for 10 min each in solution I containing 0.25% Triton, 10 mM EDTA, 1 mM EGTA, and 10 mM HEPES (pH 7.5), and in solution II containing 0.2 M NaCl, 1 mM EDTA, 1 mM EGTA, and 10 mM HEPES (pH 7.5). Extracts were obtained by 8 × 15 s sonication in lysis buffer containing 1% SDS and 10 mM EDTA using a Fisher Scientific Model 550 sonicator at setting 4 with a microtip. Chromatin was purified from insoluble debris by microcentrifugation at 15,000 rpm for 20 min.

To perform immunoprecipitation, the chromatin was diluted 1:7 in dilution buffer containing 70 mM HEPES (pH 7.5), 2.5 mM NaCl, 1.5 mM EDTA, 1.5% Triton, and 0.6% deoxycholate. The extracts were precleared with preimmune IgG together with Sepharose A or G agarose beads (Amersham, Piscataway, NJ) for 1 h at 4°C. Precleared extracts were incubated with 4–6 μg of specific antibodies at 4°C overnight followed by incubation with 30 μl of agarose A or G beads for 1 h the next day. The antibodies included the N20 and C19 AR antibodies from Santa Cruz Biotech, the pol II CTD8WG16 monoclonal from QED Bioscience (San Diego, CA), and a TFIIB antibody generated in our laboratory. The beads were washed twice with buffer containing 50 mM HEPES (pH 7.5), 0.15 M NaCl, 1 mM EDTA, 1% Triton, 0.5% deoxycholate and 0.15% SDS followed by wash with LNDET buffer containing 0.25 M LiCl, 1% NP40, 1% sodium deoxycholate, 1 mM EDTA, and 10 mM Tris (pH 8.0). The protein-DNA complexes were then eluted from the beads with 30–50 μl elution buffer containing 1% SDS and 1 mM $NaHCO_3$. The eluates were diluted with 10 mM Tris (pH 8.0)-1 mM EDTA and incubated at 65°C overnight to reverse the cross-link. The samples were then treated with proteinase K at 100 ng/μl and RNAase A for 1 h at 55°C, and then extracted with phenol. The DNA was then precipitated with ethanol, resuspended in 30 μl water, and subjected to PCR analysis. Typically one 1-cm tumor yielded enough material for six PCR reactions. The input sample in the data shown in the ChIP experiments was typically 2% of the DNA added to a ChIP reaction.

The PCR analyses were performed with four sets of ^{32}P-labeled of primers: Enhancer: 5′ggtgaccagagcagtctaggtg3′ and 5′tgtttactgtcaaggacaatcgat3′; Promoter: 5′gtatgaagaatcggggatcgt3′ and 5′ gctcatggagacttcatctag3′; Middle: 5′tatgcttggggacaccggat3′ and 5′ttagagctggagtggaaggatat3′; Exon 5: 5′taatggtgtgcttcaaggtatcacg3′ and 5′gtgtccttgatccacttccggtaat3′

The PCR cycling protocol was 40 s at 94°C, 3 min at 75°C, 2 min at 65°C, followed by 20 cycles of 40 s at 94°C, 1 min at 65°C, and 2 min at 72°C, followed by a 10-min extension at 72°C. The PCR products were phenol-extracted, separated on 6% polyacrylamide gels, and autoradiographed by exposure to XAR-5 film.

RESULTS

AdTSTA Is AR-responsive in Cell-based Assays. The transcriptional activity of AR is the most relevant measure of its function *in vivo*. Our previous study used a plasmid expressing the TSTA system to study AR-mediated gene expression in cell culture (46). To monitor AR in live animal models of prostate cancer it was necessary to insert the TSTA cassette (Fig. 1*A*) into an adenovirus, which could be injected directly into tumors. The cassette was inserted into the

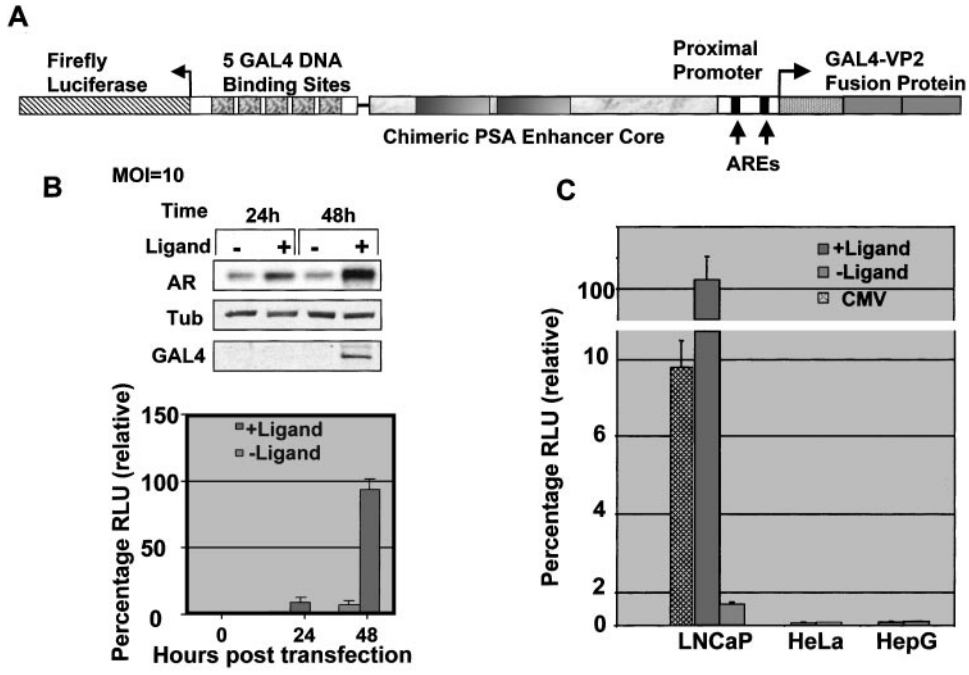

Fig. 1. Validation of the molecular imaging system in cell culture. *A*, a schematic of the AdTSTA imaging system. The *top portion* of the diagram shows the TSTA imaging cassette. The PSA enhancer from −4326 to −3935 was duplicated (the chimeric enhancer core) within the upstream regulatory region from −5322 to −3744 and attached to the proximal promoter from −541 to 1. Each enhancer bears a cluster of six AREs, and the promoter contains two AREs. The PSA regulatory region is shown expressing GAL4-VP2 bearing two NH_2-terminal herpes simplex virus 1 VP16 activation domains (amino acids 413–454) fused to the GAL4 DNA binding domain (amino acids 1–147). A GAL4-responsive promoter is fused in the divergent orientation to the PSA regulatory region. The GAL4-responsive promoter contains five 17-bp GAL4 sites upstream of the adenovirus E4 promoter driving firefly luciferase. The entire cassette was cloned into a shuttle vector and introduced into Ad5 deleted (△) for E1 and E3 using the AdEasy system. The virus was propagated in 293 cells, purified and titered. *B*, a demonstration of AdTSTA activity in cancer cell lines. LNCaP cells were infected with AdTSTA at a MOI of 10 for 1 h and treated with 10 nM R1881 (+*Ligand*) or vehicle (−*Ligand*). At the indicated time points, the cells were lysed with Reporter Lysis Buffer, and firefly luciferase activity was analyzed either by luminometry (*bottom panel*, *Y*-axis: Relative Luciferase Units/μg of total protein normalized to 100%) or by immunoblotting (*top panel*, *AR*, anti-AR; *Tub*, Anti-tubulin; GAL4, anti-GAL4-VP16). Samples were prepared in triplicate and the average reading is shown; *bars*, ±SE. The triplicate samples were mixed for immunoblot analysis. *C*,. LNCaP, HeLa, or HepG cells were infected with AdTSTA at a MOI of 0.1 for 1 h followed by treatment with 10 nM R1881. The cells were harvested 48 h later, and luciferase levels were measured. Data are normalized to the ligand-induced signal in LNCaP (100%). The AdCMV (MOI 0.1) signal in LNCaP is shown in ▨ for comparison of the AdTSTA and AdCMV luciferase activity; *bars*, ±SE.

genome of adenovirus serotype 5 in which the E1 and E3 coding regions were deleted, which rendered the virus replication-deficient (47). The TSTA cassette comprises a modified PSA regulatory region containing two copies of the AR-responsive core PSA enhancer placed upstream of GAL4-VP2. GAL4-VP2 contains two copies of the VP16 activation domain fused to the GAL4 DNA binding domain. In the presence of androgen, GAL4-VP2 is synthesized and binds to five GAL4 binding sites positioned upstream of the adenovirus E4 core promoter, which drives high levels of firefly luciferase expression (Fig. 1). Luciferase was measured in cell culture by luminometry and *in vivo* in D-luciferin-injected live animals using a Xenogen cooled CCD optical imaging system (42).

To validate the androgen responsiveness of the TSTA system in the context of the adenoviral vector, we infected the model AD prostate cancer cell line, LNCaP, with AdTSTA (Fig. 1*B*). GAL4-VP2 and firefly luciferase levels were enhanced significantly in the presence of the synthetic androgen agonist R1881. The largest increase of luciferase activity was observed at the 48-h time point (Fig. 1*B*, *bottom*), which correlated with the appearance of GAL4-VP2 by immunoblot analysis (Fig. 1*B*, *top*).

The AdTSTA system maintained cell selectivity in culture (Fig. 1*C*). An example of these findings is shown for cells derived from prostate cancer (LNCaP), liver (HepG), and cervical cancer (HeLa). LNCaP is an AD prostate cancer cell line (49), which contains a mutant form of AR and secretes PSA (50, 51). AR expression is not observed in HeLa and HepG cells (data not shown). PCR analysis demonstrated that viral infectivity was similar within a 2-fold range among the cell lines tested (data not shown). The LNCaP cells displayed significantly higher firefly luciferase activity than HeLa and HepG, and responded to the androgen agonist R1881. MCF-7 cells (an AR-expressing breast cancer cell line), PC3 (an AR-negative prostate cancer cell line), and PC3 stably expressing AR were also tested. These lines displayed only a low basal level of TSTA expression and did not respond to R1881 (data not shown). Thus, the AdTSTA system responds to AR in AD prostate cancer cells. The residual signal present in LNCaP cells in the absence of ligand could be suppressed by addition of the AR antagonist casodex suggesting that the TSTA amplification system is sensitive enough to respond to trace androgen levels present in charcoal-stripped growth medium (data not shown).

The AdTSTA also achieved an activity level suitable for dynamic measurements in live animals. Side-by-side comparison in LNCaP cells demonstrated that AdTSTA displayed a ligand-induced firefly luciferase activity 10-fold greater than AdCMV (Fig. 1*C*) and nearly 200-fold greater than AdPBC (data not shown). The increased activity obtained by using the TSTA approach reduced the average CCD acquisition times from 5 min to a few seconds (*i.e.*, *versus* AdPBC). The signal obtained from AdTSTA was tumor specific and robust. Direct intratumoral injection into LAPC9 AD xenografts demonstrated that AdTSTA was routinely twice as active as AdCMV. Additionally, AdTSTA, unlike AdCMV, did not generate a CCD signal in liver when injected via the tail vein into nontumor bearing SCID mice (Supplementary Fig. 2). The gain in signal obtained via the use of TSTA permitted us to perform direct measurements of AR function at various stages of cancer growth. The high level of activity also allowed us to reduce the viral dose from 10^9 pfu used in the AdPBC study to 10^7 pfu used here. The lower doses decrease the possibility of viral toxicity.

Molecular Imaging of AR Signaling in AD, ADc, and AI Tumors. To demonstrate the androgen responsiveness of the tumor model we first castrated male mice bearing LAPC9 AD tumors and measured serum PSA levels (Fig. 2). A decrease or plateau of serum PSA is indicative of successful hormone blockade therapy in humans.

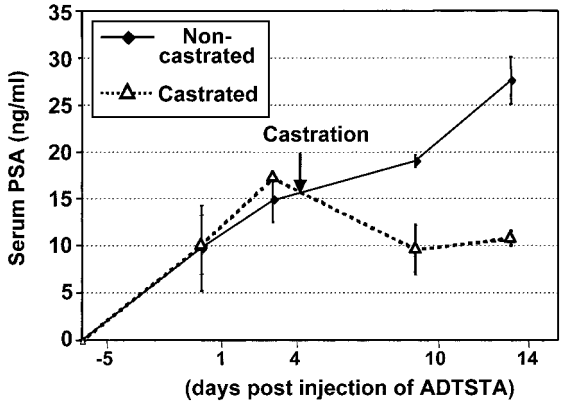

Fig. 2. Serum PSA measurements for AD and castrated mice. Serum ELISA measurements of PSA at various time points during tumor growth. Values are in ng/ml; *bars*, ±SE.

The xenograft data revealed that the PSA levels ceased rising and dropped slightly beginning 1 day after castration and remained flat, recapitulating the clinical response to androgen blockade therapy. At later time points, the PSA levels began to rise as tumors transitioned from AD to AI. Like PSA, the serum DHT levels decreased after castration to as low as 85% of the intact animals. However, DHT levels remained low even as PSA levels increased (data not shown).

Analysis of normal AD animals and animals castrated during tumor growth (ADc) revealed that the CCD imaging signal responded well to androgen withdrawal (Fig. 3*A*). The AdTSTA-injected AD tumors typically emitted $>10^7$ photons/sec/cm^2/sr on day 4 after virus injection. Castration on day 4 led to a >10-fold drop in the imaging signal by day 10 (Fig. 3*A graphs*; AD *versus* ADc; $P = 0.01$). In contrast, AdTSTA displayed robust activity in established AI tumors, and over the same time frame the signal increased. The increasing signal in AI *versus* AD tumors was intriguing, but we do not yet understand the cause. We have noted that AD tumors contain a large necrotic center, whereas AI tumors do not. It is plausible that the necrosis leads to some diminution in signal because of death of a subset of infected cells. Nevertheless, we can conclude from these data that the AR-responsive TSTA system is specifically responding to the loss of AR activity in the ADc tumor but that the activity is regained in established AI tumors.

Localization of AR in Tumors. The distribution of AR is sensitive to androgen depletion. AR is known to localize predominantly to the nucleus in the presence of androgen, whereas AR localization in the absence of androgen is diffuse, and distributes between the cytoplasm and nucleus (22). Immunohistochemical analyses of tumors from the sacrificed LAPC9 animals used in the imaging studies showed that AR was tightly localized to the nucleus of AD and established AI tumors (Fig. 3*B*). Typically 30–35% of the cells in the field stained strongly for nuclear AR, ~20% stained weakly, and the remainder displayed marginal or no staining in both AD and recurrent tumors. The staining in ADc was heterogeneous with a few cells showing nuclear staining but most showing a diffuse pattern of cytoplasmic staining.

The imaging and cytology data imply that AR initially ceases activity on castration probably because it exits the nucleus. However, AR resumes functioning in AI cancer. Several proposals have been made to explain how androgen-responsive genes could be activated in cells lacking physiological levels of androgen. In one model, other transcription factors like nuclear factor κB have been proposed to bind regulatory regions of androgen-responsive genes and partly substitute for AR in AI cancer (52). Nevertheless, the predominant nuclear location of AR in AI tumors implies that AR is functional. One

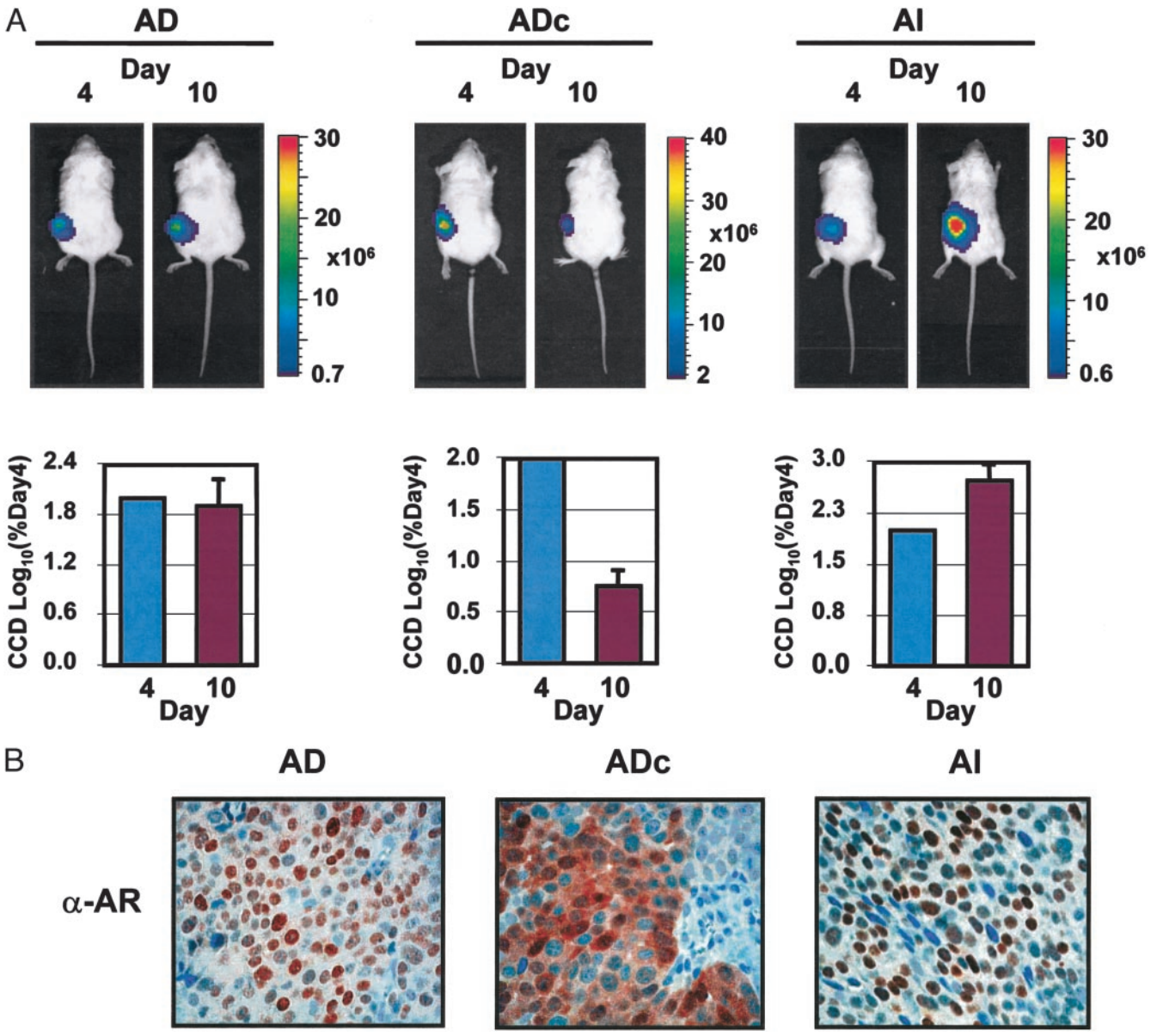

Fig. 3. Imaging AR signaling in LAPC 9 tumors. In *A*, SCID mice implanted with LAPC9 xenografts (>0.5 cm) were injected with 10^7 pfu of AdTSTA and the mice were imaged every 3–4 days until day 14. Representative mice at day 4 and day 10 after virus injection from the AD group, the castrated (on day 4) AD group (*ADc*), and the stable AI group. The *bar graph* summarizes a cohort of three or more and summarizes the log of the percentage change in signal from day 4 (*blue bars*) to day 10 (*purple bars*). Day 4 is set at 2 (*log 10*) in each case. The normalization to percentage change was necessary because there is variation in virus infectivity in different tumors. *B* shows representative immunohistochemical localization of AR in the AD, ADc, and AI tumors using anti-AR antibodies. AR stains *brown* against the blue-stained nuclei. For both AD and AI tumors, five high-power fields (×40) from multiple sample slides were counted, with an average of 100 cells/field. AR nuclear staining was recorded as percentage of cells counted. For AD tumors, cells with high AR nuclear staining are 33% (±5%), whereas cells with no or very faint AR nuclear staining is 19% (±6%) with the remainder staining at an intermediate intensity. For AI tumors, 30% (±2.7%) of the cells stained intensely, whereas cells with no or very faint AR nuclear staining was 22% (±3%). In conclusion, AR nuclear staining does not differ significantly between AD and AI tumors ($P = 0.3$ one tail and 0.7 two tail); *bars*, ±SE.

prediction of this hypothesis is that AR should bind directly to responsive enhancers and promoters in AI tumors.

Transcription Complex Assembly in Tumors. To determine whether AR was binding to the endogenous PSA regulatory region in AI tumors we used ChIP, which allows direct measurement of DNA binding to promoters and enhancers *in vivo* (Fig. 4). Previous ChIP experiments in AD LNCaP cells in culture have shown that AR and pol II bind to the PSA enhancer and promoter when the gene is active (15, 17). We analyzed AR binding to four regions of the gene in tumors: the enhancer, the promoter, an intervening region located between the enhancer and promoter, and downstream exon 5 (Fig. 4, *schematic*). Specific signals were confirmed by comparing the AR antibody signal to the background observed in a mock immunoprecipitation with IgG.

AR binding to both the PSA enhancer and promoter in the AD samples was detectable well above the IgG background (Fig. 4, *autoradiographs*). AR binding to the enhancer and promoter was specific because it was minimal within the middle intervening region and exon 5. Remarkably, AR bound nearly as well to the promoter and enhancer in the AI samples, demonstrating that it was fully functional in the presence of androgen withdrawal in a recurrent tumor.

The ChIP results were consistent when normalized to the signal from input DNA and averaged among three experiments. The binding of AR to the enhancer in AI tumors was typically only 20% lower than in AD tumors (Fig. 4, *graph*). In contrast, on ADc the binding of AR to the enhancer and promoter decreased 4-fold. There is still evidence of specific AR binding in ADc, because the signals on the enhancer and promoter are above the IgG background. The residual binding can

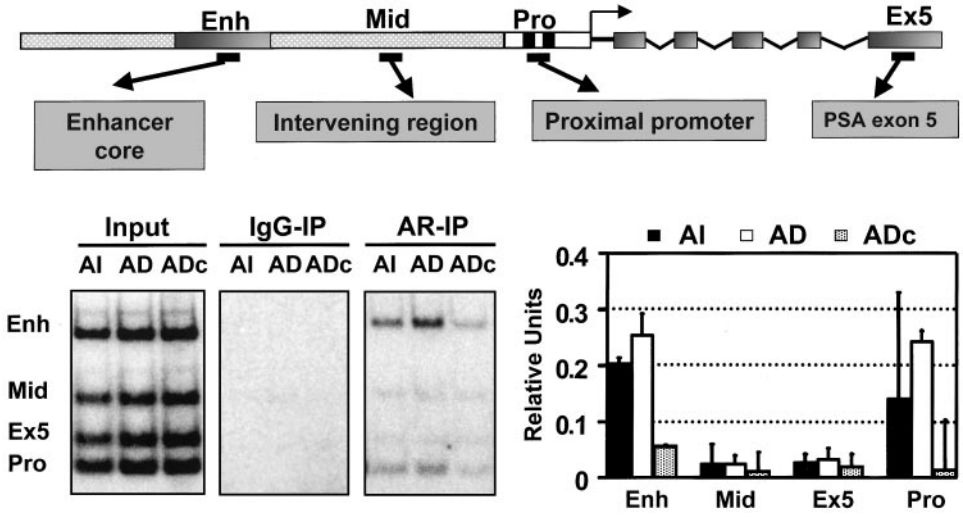

Fig. 4. Chromatin immunoprecipitation assays in LAPC9 tumors. The diagram in the *top panel* describes the PSA regulatory region. *Short black line underneath* indicates the positions targeted by PCR. *Enh*, enhancer core; *Mid*, intervening region; *Pro*, proximal promoter; *Ex5*, PSA exon 5 (for sequence coordinates see "Materials and Methods"). Tumors were isolated from mice sacrificed at day 10 (6 days after castration for ADc), minced, cross-linked with formaldehyde, and immunoprecipitated with anti-AR or a IgG (mock). Autoradiographs of the multiplex PCR reactions are shown for AD, AI, and ADc tumors. Input represents 2% of the DNA added to the immunoprecipitation reaction. Graph of multiple tumor ChIP analyses. The band intensities were analyzed using ImageQuant. Background values from a mock (IgG) ChIP were subtracted from each band and normalized to the signal from input DNA. *Bars*, ±SD of three values obtained in independent experiments.

be explained in part by the cytology data in which some AR remains in the nucleus even in ADc. Additionally, the PSA levels and imaging signals do not decrease to baseline in ADc but drop transiently as the tumor begins to transition to AI. This suggests that a small amount of residual AR-dependent PSA gene transcription occurs in the presence of castrate levels of ligand.

We initiated a mechanistic study to examine how transcription complexes respond to the presence and absence of hormone. We began by analyzing pol II, which should be found in both promoter-bound and elongating positions when the PSA gene is transcriptionally active (Fig. 5). Elongating pol II was measured by its binding to exon 5, which is easily discriminated from its binding to the promoter. As predicted, pol II binding was observed at both the promoter and downstream exon 5 in the AD and AI tumors. However, the ratio of the signal at exon 5 *versus* the proximal promoter shows that in AD and AI tumors pol II is primarily localized at exon 5.

Remarkably, in ADc tumors after castration, pol II remained bound to the gene at levels similar to those seen in AD tumors. However, pol II was positioned primarily at the promoter instead of exon 5 (Fig. 5, *top*, compare ratio of exon 5 to promoter). The overall amounts of the general factor TFIIB present at the PSA promoter also did not change in AD, ADc, and AI. Our interpretation of these findings is that the transcription complex remains intact after androgen deprivation, but a greater fraction of pol II is not actively transcribing in ADc *versus* AD and AI. A scatter plot summarizing four representative experiments is shown in Supplementary Data Fig. 2.

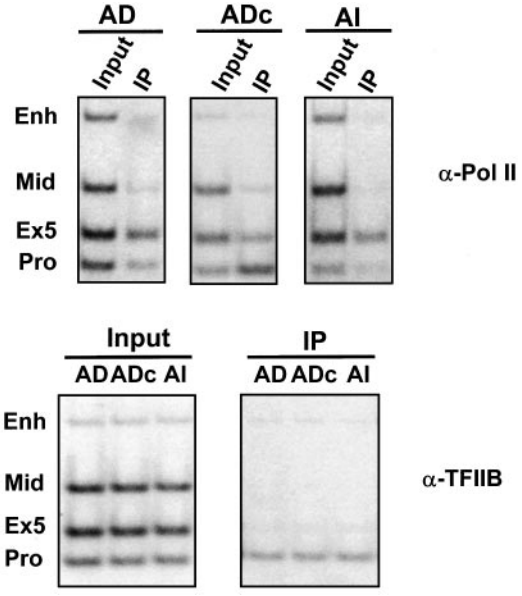

Fig. 5. ChIP analysis of RNA polymerase II and TFIIB from LAPC9 tumors. The bands are described in the Fig. 6 legend. Representative experiments from AD, AI, and ADc tumors are shown. The *top panels* are pol II, and the *bottom panels* are TFIIB.

Visualizing the AD-AI Transition. The original goal in developing the TSTA system was to monitor the loss and gain of AR-mediated transcription over time in a single individual as a tumor transitioned from ADc to AI. In a human, the failure of androgen deprivation therapy occurs gradually over a period of time that can vary from weeks to years. The LAPC9 models were originally adapted to an androgen-rich environment in immunodeficient male mice and then trained to grow in an AI manner in castrate or female mice, a process that can take months. However, we have found that the transition from AD to recurrent growth occurs rapidly as the tumor grows larger. In some animals the transition occurs quickly enough to monitor it over a short period of time as opposed to studying established AI tumors. The data in Fig. 6 illustrate a typical example of an animal undergoing the transition.

In this animal, we injected the AdTSTA virus, imaged 4 days later, and then castrated the animal when the tumor reached 1 cm. We observed that the PSA levels initially dropped up to 2.4-fold by day 10, 6 days postcastration, and then began rising again up to day 17. Over this same time frame, the imaging signal was high on day 4, reached a minimum by day 10, and then gradually rose again by day 17 (Fig. 6, *top*).

ChIP and immunohistochemical analyses on the tumor from the sacrificed animal revealed that AR resumed its nuclear localization and was bound primarily to the PSA enhancer, whereas pol II was found predominantly in the elongating state at exon 5 (Fig. 6, *bottom*). In short, we show an example where AR has adapted to the androgen-deprived environment and resumed activity in the AI state as measured by gene expression-based imaging, immunohistochemistry, and ChIP.

DISCUSSION

AR Function in Recurrent Cancer. The natural response of prostate cancer to DHT withdrawal is transition to the recurrent state. In men, localized cancer can be treated surgically, but metastasized cancers become refractory to androgen withdrawal and resume

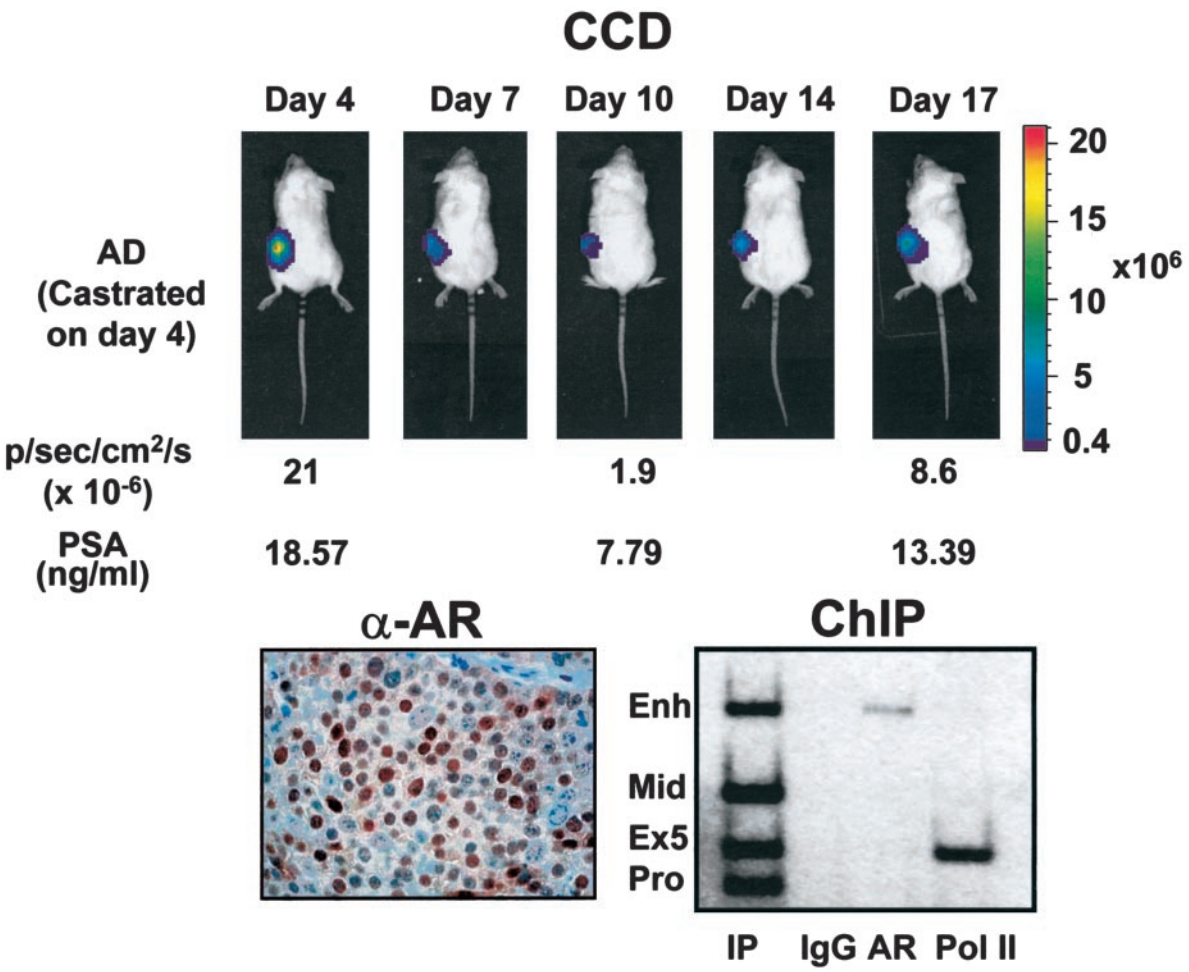

Fig. 6. Dynamic AR signaling. A SCID mouse bearing an LAPC9 AD tumor was injected with AdTSTA, imaged, and castrated. The *top panel* shows the entire time course with signals adjusted to the same color scale. Imaging measurements and PSA levels determined by serum ELISA are shown below the images. *Bottom left panel,* the tumors were extracted and subjected to immunohistological staining with AR antibodies. *Bottom right panel,* a ChIP assay of the extracted tumors with IgG, AR and pol II antibodies.

growth. The ability to recapitulate the transition to the recurrent state in xenograft models has provided a powerful tool for studying prostate tumor biology. The xenograft animals display the typical loss and then rise again in PSA levels upon castration. Although PSA is an AR-regulated gene, there have been proposals that other transcription factors may substitute for AR or that AR may be activating genes by a nongenotropic mechanism.

Three observations argue for a direct restoration of AR function. First, we redesigned the PSA transcriptional regulatory region to dramatically increase its response to AR. The modified PSA regulatory region was then built into a TSTA cassette to amplify its potency for use in live animal imaging. The imaging signals in recurrent tumors strongly suggest that AR is fully active. Furthermore, we could monitor the transition of an AD tumor to a recurrent state in a single individual, and visualize the loss and gain of AR activity during tumor progression. Second, immunohistochemistry on the xenograft tumors showed that AR localization was diffuse on androgen withdrawal but became tightly localized to the nucleus in recurrent tumors consistent with its role in DNA binding and transactivation. Finally, AR bound directly to the regulatory region of the PSA gene of AD tumors as measured by ChIP. Although the bulk of AR dissociated on castration it rebound again in stable AI and recurrent tumors. This last observation is particularly significant, because direct AR binding to a prostate-expressed gene has not been shown yet in advanced cancer.

Molecular Imaging of Prostate Cancer. The TSTA imaging scheme is a powerful approach to amplify weak cell-specific promoters and monitor their activity in live animals. By cloning the PSA-based TSTA cassette into adenovirus we generated a tool to monitor AR function during tumor progression from the AD to recurrent state. The AdTSTA system was designed to be particularly sensitive to AR by manipulating the enhancer region, which binds multiple molecules of AR cooperatively. The system responded dynamically and sensitively to castration of tumor-bearing mice. Typically, imaging signals decreased more rapidly than PSA levels, and the magnitude of the decrease was greater with the imaging system (10–20-fold) than PSA (2–3-fold). The short half-life of firefly luciferase (~12 h in the tumor) and the fact that it is an intracellular protein may have contributed to the enhanced sensitivity of the imaging signal. PSA is a secreted protein that exists both in the cell and serum. PSA half-life and secretion rates are likely to respond variably to the tumor environment and may not provide an immediate measure of AR activity.

The TSTA system is versatile and modular. We have now completed cloning of shuttle vectors in which the reporter gene can be replaced by any reporter (*e.g.,* thymidine kinase, green fluorescent protein, or *renilla* luciferase) or therapeutic gene for imaging or gene therapy. Furthermore, although we chose the modified PSA enhancer in our studies, the vector can accommodate any cell-specific or viral promoter. Finally, the system is titratable. In our previous cell culture study, which used plasmids, we systematically varied both the number of VP16 activation domains attached to GAL4 or the number of GAL4 sites driving the reporter. We were able to achieve a range of activities over 3 orders of magnitude. This variation should allow

optimization of signal:noise ratios and amplification of weak promoters for any application. Additionally, the vector is designed to replace the VP16 activation domain with domains that respond to signal transduction cascades. For example, we have successfully replaced VP16 with the activation domain of Elk-1 and shown that the system responds in a binary fashion to AR and signals emanating from the MAPK cascade.

On a technical note, there may be concerns about GAL4-VP16 and firefly luciferase toxicity. However, if toxicity was a significant issue we would predict that infected cells would die rapidly and the imaging signal would decay. However, under the conditions used in our study we were able to obtain persistent imaging signals in tumors over the course of the experiments, which can last up to a month. Also, the virus is not unusually toxic in cell culture, where cells appear to divide after infection. Our ability to use low doses of virus in the animal studies may permit a less immunogenic response and enable us to transit the system into non-SCID prostate models and transgenic animals.

Mechanism of AR Activation. The mechanism by which AR is reactivated in tumors has been the subject of much research and is commented on in the "Introduction." There are several interconnected issues including how does AR localize to the nucleus in the presence of castrate amounts of ligand, and how does it bind DNA and function in such an environment?

AR overexpression, ligand-binding domain mutations, and MAPK signaling have all been proposed as possible mechanisms to facilitate AR translocation and activity. Overexpression of SRC-1 and -2 coactivators has also been observed in some prostate tumors and may facilitate AR function. We have made two observations that bear on this issue. First, the AR levels in our recurrent tumors, when normalized to β-tubulin using a human specific antibody, are not dramatically higher than those in AD tumors (Supplementary Data, Fig. 3). We have also measured SRC-1, -2, and -3 levels, and they vary less than a few-fold among LAPC9 cancers. Thus, the localization of AR to the nuclei of recurrent tumors is not because of overexpression, which may bypass the normal cell trafficking checkpoints. Second, the AR gene in the LAPC9 tumor model has been sequenced and does not contain mutations in the ligand-binding domain, which might permit use of alternative ligands. Furthermore, if somehow the tumors were adapting to castration by hyperactivating pathways that convert adrenal androgen to DHT, we would have expected to see gradual increases in serum DHT over time. However, circulating levels of DHT in the LAPC9 mice drop up to 85% immediately after castration and remain at castrate levels throughout tumor growth. Finally, it is plausible that MAPK pathways are influencing AR translocation. We note that the particular tumor model we use, LAPC9, has been shown to display elevated EGF receptor and MAPK signaling (31).

Transcription Complex Assembly by AR. The binding of AR to the PSA enhancer paralleled increased serum PSA levels, the imaging signal, and AR cellular localization in both AD and AI cancer. Although AR-enhancer binding decreased 4-fold in ADc it increased again in AI cancer. As mentioned previously, PSA levels do not disappear completely in ADc but transiently plateau or drop as the tumors adapt. This observation can be explained by the fact that a subset of tumor cells from castrated animals still display AR nuclear localization and residual AR binding to the enhancer.

Although our data do not illuminate the precise mechanism of AR reactivation they provide insight into how the AD-AI transition may be facilitated. The most intriguing result is that although castration causes 75% of AR to dissociate from the PSA enhancer, the levels of bound TFIIB and pol II remain unchanged. However, castration did result in redistribution of pol II from exon 5 to the promoter. These observations suggest that transcription complexes do not disappear but remain poised to facilitate reactivation of AR-mediated transcription.

AR and pol II are known to cycle on and off the promoter during gene activation in LNCaP cells (15, 17). The peaks of AR and subsequent pol II binding after androgen addition do not coincide, suggesting that AR can leave while pol II is engaging the promoter. Analysis of genes such as α1-AT have also established that pol II can be bound with general factors such as TFIIB in a quiescent state, before binding of the activator (53). These data along with older studies of the heat shock locus in *Drosophila* (54) indicate that a prepoised pol II may provide a mechanism for maintaining promoter accessibility during a transcriptionally inactive state. The factors that control pol II redistribution are unknown. However, mutations in forkhead transcription factors in yeast are known to cause redistribution of pol II to the promoter (55). It is plausible that the poised complexes may be sensitive to lower levels of functional AR, thereby allowing activation in the absence of physiological levels of DHT. We are currently pursuing the mechanism of this effect.

ACKNOWLEDGMENTS

We thank Erika Billick for technical assistance during the early stages of the study, and Charles Sawyers and his laboratory for helpful discussions.

REFERENCES

1. Gelmann, E. P. Molecular biology of the androgen receptor. J. Clin. Oncol., *20:* 3001–3015, 2002.
2. Freedman, L. P. Increasing the complexity of coactivation in nuclear receptor signaling. Cell, *97:* 5–8, 1999.
3. Waller, A. S., Sharrard, R. M., Berthon, P., and Maitland, N. J. Androgen receptor localisation and turnover in human prostate epithelium treated with the antiandrogen, casodex. J. Mol. Endocrinol., *24:* 339–251, 2000.
4. Tyagi, R. K., Lavrovsky, Y., Ahn, S. C., Song, C. S., Chatterjee, B., and Roy, A. K. Dynamics of intracellular movement and nucleocytoplasmic recycling of the ligand-activated androgen receptor in living cells. Mol. Endocrinol., *14:* 1162–1174, 2000.
5. Bok, R. A., and Small, E. J. Bloodborne biomolecular markers in prostate cancer development and progression. Nat. Rev. Cancer, *2:* 918–926, 2002.
6. Pang, S., Taneja, S., Dardashti, K., Cohan, P., Kaboo, R., Sokoloff, M., Tso, C. L., Dekernion, J. B., and Belldegrun, A. S. Prostate tissue specificity of the prostate-specific antigen promoter isolated from a patient with prostate cancer. Hum. Gene Ther., *6:* 1417–1426, 1995.
7. Pang, S., Dannull, J., Kaboo, R., Xie, Y., Tso, C. L., Michel, K., deKernion, J. B., and Belldegrun, A. S. Identification of a positive regulatory element responsible for tissue- specific expression of prostate-specific antigen. Cancer Res., *57:* 495–499, 1997.
8. Schuur, E. R., Henderson, G. A., Kmetec, L. A., Miller, J. D., Lamparski, H. G., and Henderson, D. R. Prostate-specific antigen expression is regulated by an upstream enhancer. J. Biol. Chem., *271:* 7043–7051, 1996.
9. Cleutjens, K. B., van Eekelen, C. C., van der Korput, H. A., Brinkman, A. O., and Trapman, J. Two androgen response regions cooperate in steroid hormone regulated activity of the prostate-specfic antigen promoter. J. Biol. Chem., *271:* 6379–6388, 1996.
10. Cleutjens, K. B., van der Korput, H. A., van Eekelen, C. C., van Rooij, H. C., Faber, P. W., and Trapman, J. An androgen response element in a far upstream enhancer region is essential for high, androgen-regulated activity of the prostate-specific antigen promoter. Mol. Endocrinol., *11:* 148–161, 1997.
11. Cleutjens, K. B., van der Korput, H. A., Ehren-van Eekelen, C. C., Sikes, R. A., Fasciana, C., Chung, L. W., and Trapman, J. A 6-kb promoter fragment mimics in transgenic mice the prostate-specific and androgen-regulated expression of the endogenous prostate-specific antigen gene in humans. Mol. Endocrinol., *11:* 1256–1265, 1997.
12. Zhang, S., Murtha, P. E., and Young, C. Y. Defining a functional androgen responsive element in the 5′ far upstream flanking region of the prostate-specific antigen gene. Biochem. Biophys. Res. Commun., *231:* 784–788, 1997.
13. Huang, W., Shostak, Y., Tarr, P., Sawyers, C., and Carey, M. Cooperative assembly of androgen receptor into a nucleoprotein complex that regulates the prostate-specific antigen enhancer. J. Biol. Chem., *274:* 25756–25768, 1999.
14. Reid, K. J., Hendy, S. C., Saito, J., Sorensen, P., and Nelson, C. C. Two classes of androgen receptor elements mediate cooperativity through allosteric interactions. J. Biol. Chem., *276:* 2943–2952, 2001.
15. Kang, Z., Pirskanen, A., Janne, O. A., and Palvimo, J. J. Involvement of proteasome in the dynamic assembly of the androgen receptor transcription complex. J. Biol. Chem., *277:* 48366–48371, 2002.
16. Louie, M. C., Yang, H. Q., Ma, A. H., Xu, W., Zou, J. X., Kung, H. J., and Chen, H. W. Androgen-induced recruitment of RNA polymerase II to a nuclear receptor-p160 coactivator complex. Proc. Natl. Acad. Sci. USA, *100:* 2226–2230, 2003.

17. Shang, Y., Myers, M., and Brown, M. Formation of the androgen receptor transcription complex. Mol. Cell, *9:* 601–610, 2002.
18. Lee, C. T., and Oesterling, J. E. Diagnostic markers of prostate cancer: utility of prostate-specific antigen in diagnosis and staging. Semin. Surg. Oncol., *11:* 23–35, 1995.
19. Abate-Shen, C., and Shen, M. M. Molecular genetics of prostate cancer. Genes Dev., *14:* 2410–2434, 2000.
20. Arnold, J. T., and Isaacs, J. T. Mechanisms involved in the progression of androgen-independent prostate cancers: it is not only the cancer cell's fault. Endocr. Relat. Cancer, *9:* 61–73, 2002.
21. Feldman, B. J., and Feldman, D. The development of androgen-independent prostate cancer. Nat. Rev. Cancer, *1:* 34–45, 2001.
22. Gregory, C. W., Johnson, R. T., Jr., Mohler, J. L., French, F. S., and Wilson, E. M. Androgen receptor stabilization in recurrent prostate cancer is associated with hypersensitivity to low androgen. Cancer Res., *61:* 2892–2898, 2001.
23. Visakorpi, T., Hyytinen, E., Koivisto, P., Tanner, M., Keinanen, R., Palmberg, C., Palotie, A., Tammela, T., Isola, J., and Kallioniemi, O. P. *In vivo* amplification of the androgen receptor gene and progression of human prostate cancer. Nat. Genet., *9:* 401–406, 1995.
24. Stanbrough, M., Leav, I., Kwan, P. W., Bubley, G. J., and Balk, S. P. Prostatic intraepithelial neoplasia in mice expressing an androgen receptor transgene in prostate epithelium. Proc. Natl. Acad. Sci. USA, *98:* 10823–10828, 2001.
25. Gregory, C. W., He, B., Johnson, R. T., Ford, O. H., Mohler, J. L., French, F. S., and Wilson, E. M. A mechanism for androgen receptor-mediated prostate cancer recurrence after androgen deprivation therapy. Cancer Res., *61:* 4315–4319, 2001.
26. Han, G., Foster, B. A., Mistry, S., Buchanan, G., Harris, J. M., Tilley, W. D., and Greenberg, N. M. Hormone status selects for spontaneous somatic androgen receptor variants that demonstrate specific ligand and cofactor dependent activities in autochthonous prostate cancer. J. Biol. Chem., *276:* 11204–11213, 2001.
27. Grossmann, M. E., Huang, H., and Tindall, D. J. Androgen receptor signaling in androgen-refractory prostate cancer. J. Natl. Cancer Inst., *93:* 1687–1697, 2001.
28. Craft, N., and Sawyers, C. L. Mechanistic concepts in androgen-dependence of prostate cancer. Cancer Metastasis Rev., *17:* 421–427, 1998.
29. Elo, J. P., and Visakorpi, T. Molecular genetics of prostate cancer. Ann. Med., *33:* 130–141, 2001.
30. Gioeli, D., Mandell, J. W., Petroni, G. R., Frierson, H. F., Jr., and Weber, M. J. Activation of mitogen-activated protein kinase associated with prostate cancer progression. Cancer Res., *59:* 279–284, 1999.
31. Mellinghoff, I. K., Tran, C., and Sawyers, C. L. Growth inhibitory effects of the dual ErbB1/ErbB2 tyrosine kinase inhibitor PKI-166 on human prostate cancer xenografts. Cancer Res., *62:* 5254–5259, 2002.
32. Zegarra-Moro, O. L., Schmidt, L. J., Huang, H., and Tindall, D. J. Disruption of androgen receptor function inhibits proliferation of androgen-refractory prostate cancer cells. Cancer Res., *62:* 1008–1013, 2002.
33. Kousteni, S., Bellido, T., Plotkin, L. I., O'Brien, C. A., Bodenner, D. L., Han, L., Han, K., DiGregorio, G. B., Katzenellenbogen, J. A., Katzenellenbogen, B. S., Roberson, P. K., Weinstein, R. S., Jilka, R. L., and Manolagas, S. C. Nongenotropic, sex-nonspecific signaling through the estrogen or androgen receptors: dissociation from transcriptional activity. Cell, *104:* 719–730, 2001.
34. Peterziel, H., Mink, S., Schonert, A., Becker, M., Klocker, H., and Cato, A. C. Rapid signalling by androgen receptor in prostate cancer cells. Oncogene, *18:* 6322–6329, 1999.
35. Yeung, F., Li, X., Ellett, J., Trapman, J., Kao, C., and Chung, L. W. Regions of prostate-specific antigen (PSA) promoter confer androgen- independent expression of PSA in prostate cancer cells. J. Biol. Chem., *275:* 40846–40855, 2000.
36. Klein, K. A., Reiter, R. E., Redula, J., Moradi, H., Zhu, X. L., Brothman, A. R., Lamb, D. J., Marcelli, M., Belldegrun, A., Witte, O. N., and Sawyers, C. L. Progression of metastatic human prostate cancer to androgen independence in immunodeficient SCID mice. Nat. Med., *3:* 402–408, 1997.
37. Contag, C. H., Jenkins, D., Contag, P. R., and Negrin, R. S. Use of reporter genes for optical measurements of neoplastic disease *in vivo*. Neoplasia, *2:* 41–52, 2000.
38. Contag, P. R. Whole-animal cellular and molecular imaging to accelerate drug development. Drug Disc. Today, *7:* 555–562, 2002.
39. Herschman, H. R., MacLaren, D. C., Iyer, M., Namavari, M., Bobinski, K., Green, L. A., Wu, L., Berk, A. J., Toyokuni, T., Barrio, J. R., Cherry, S. R., Phelps, M. E., Sandgren, E. P., and Gambhir, S. S. Seeing is believing: non-invasive, quantitative and repetitive imaging of reporter gene expression in living animals, using positron emission tomography. J. Neurosci. Res., *59:* 699–705, 2000.
40. Massoud, T., and Gambhir, S. S. Molecular imaging in living subjects: Seeing fundamental biological processes in a new light. Genes Dev., *17:* 545–580, 2003.
41. O'Connell-Rodwell, C. E., Burns, S. M., Bachmann, M. H., and Contag, C. H. Bioluminescent indicators for *in vivo* measurements of gene expression. Trends Biotechnol., *20:* S19–S23, 2002.
42. Wu, J. C., Sundaresan, G., Iyer, M., and Gambhir, S. S. Noninvasive optical imaging of firefly luciferase reporter gene expression in skeletal muscles of living mice. Mol. Ther., *4:* 297–306, 2001.
43. Wu, L., Matherly, J., Smallwood, A., Adams, J. Y., Billick, E., Belldegrun, A., and Carey, M. Chimeric PSA enhancers exhibit augmented activity in prostate cancer gene therapy vectors. Gene Ther., *8:* 1416–1426, 2001.
44. Adams, J. Y., Johnson, M., Sato, M., Berger, F., Gambhir, S. S., Carey, M., Iruela-Arispe, M. L., and Wu, L. Visualization of advanced human prostate cancer lesions in living mice by a targeted gene transfer vector and optical imaging. Nat. Med., *8:* 891–897, 2002.
45. Iyer, M., Wu, L., Carey, M., Wang, Y., Smallwood, A., and Gambhir, S. S. Two-step transcriptional amplification as a method for imaging reporter gene expression using weak promoters. Proc. Natl. Acad. Sci. USA, *98:* 14595–14600, 2001.
46. Zhang, L., Adams, J. Y., Billick, E., Ilagan, R., Iyer, M., Le, K., Smallwood, A., Gambhir, S. S., Carey, M., and Wu, L. Molecular engineering of a two-step transcription amplification (TSTA) system for transgene delivery in prostate cancer. Mol. Ther., *5:* 223–232, 2002.
47. He, T. C., Zhou, S., da Costa, L. T., Yu, J., Kinzler, K. W., and Vogelstein, B. A simplified system for generating recombinant adenoviruses. Proc. Natl. Acad. Sci. USA, *95:* 2509–2514, 1998.
48. Pfeifer, A., and Verma, I. M. Gene therapy: promises and problems. Annu. Rev. Genomics Hum. Genet., *2:* 177–211, 2001.
49. Horoszewicz, J. S., Leong, S. S., Kawinski, E., Karr, J. P., Rosenthal, H., Chu, T. M., Mirand, E. A., and Murphy, G. P. LNCaP model of human prostatic carcinoma. Cancer Res., *43:* 1809–1818, 1983.
50. Tilley, W. D., Wilson, C. M., Marcelli, M., and McPhaul, M. J. Androgen receptor gene expression in human prostate carcinoma cell lines. Cancer Res., *50:* 5382–5386, 1990.
51. Montgomery, B. T., Young, C. Y., Bilhartz, D. L., Andrews, P. E., Prescott, J. L., Thompson, N. F., and Tindall, D. J. Hormonal regulation of prostate-specific antigen (PSA) glycoprotein in the human prostatic adenocarcinoma cell line, LNCaP. Prostate, *21:* 63–73, 1992.
52. Chen, C. D., and Sawyers, C. L. NF-κ B activates prostate-specific antigen expression and is upregulated in androgen-independent prostate cancer. Mol. Cell. Biol., *22:* 2862–2870, 2002.
53. Cosma, M. Ordered recruitment: gene-specific mechanism of transcription activation. Mol. Cell, *10:* 227–236, 2002.
54. Gilmour, D. S., and Lis, J. T. RNA polymerase II interacts with the promoter region of the noninduced hsp70 gene in Drosophila melanogaster cells. Mol. Cell. Biol., *6:* 3984–3989, 1986.
55. Morillon, A., O'Sullivan, J., Azad, A., Proudfoot, N., and Mellor, J. Regulation of elongating RNA polymerase II by forkhead transcription factors in yeast. Science (Wash. DC), *300:* 492–495, 2003.